



## Aero-sol-gel synthesis and photovoltaic properties of mesoporous TiO<sub>2</sub> nanoparticles

Ji Young Ahn<sup>a,1</sup>, Ho Kyeong Cheon<sup>b,1</sup>, Whi Dong Kim<sup>a,c</sup>, Yong Jin Kang<sup>c</sup>, Jong Man Kim<sup>b</sup>, Deug Woo Lee<sup>b</sup>, Chae Yong Cho<sup>d</sup>, Yoon Hae Hwang<sup>e</sup>, Hyun-Seol Park<sup>f</sup>, Jae-Wook Kang<sup>c,\*</sup>, Soo Hyung Kim<sup>b,\*</sup>

<sup>a</sup> Department of Nano Fusion Technology, College of Nanoscience and Nanotechnology, Pusan National University, 30 Jangjeon-dong, Geumjung-gu, Busan 609-735, Republic of Korea

<sup>b</sup> Department of Nanomechatronics Engineering, College of Nanoscience and Nanotechnology, Pusan National University, 30 Jangjeon-dong, Geumjung-gu, Busan 609-735, Republic of Korea

<sup>c</sup> Korea Institute of Materials Science, 66 Sangnam-dong, Sungsan-gu, Changwon, Kyungsangnamdo 642-831, Republic of Korea

<sup>d</sup> Department of Nanomedical Engineering, College of Nanoscience and Nanotechnology, Pusan National University, 30 Jangjeon-dong, Geumjung-gu, Busan 609-735, Republic of Korea

<sup>e</sup> Department of Nanomaterials Engineering, College of Nanoscience and Nanotechnology, Pusan National University, 30 Jangjeon-dong, Geumjung-gu, Busan 609-735, Republic of Korea

<sup>f</sup> Clean Energy System Research Center, Korea Institute of Energy Research, Yuseong-gu, Daejeon 305-343, Republic of Korea

### ARTICLE INFO

#### Article history:

Received 14 November 2011

Received in revised form 26 January 2012

Accepted 2 February 2012

#### Keywords:

Mesoporous TiO<sub>2</sub> nanoparticle

Specific surface area

Dye adsorption

Aero-sol-gel process

Dye-sensitized solar cell

### ABSTRACT

Highly mesoporous TiO<sub>2</sub> nanoparticles were synthesized by using a combination of aero-sol-gel and aqueous washing processes. By varying the mass fraction of NaCl templates in the TiO<sub>2</sub>-NaCl composite nanoparticles, we examined the formation of mesoporous TiO<sub>2</sub> nanoparticles with optimized surface area and pore volume distributions. Then, the photovoltaic properties of the resulting mesoporous TiO<sub>2</sub> nanoparticles were systematically investigated by forming a photovoltaic active layer of these nanoparticles on the photoanode of dye-sensitized solar cells (DSSCs). The mesoporous TiO<sub>2</sub> nanoparticle-based DSSCs fabricated in this study showed an improved short circuit current densities and power conversion efficiencies compared to solid TiO<sub>2</sub> nanoparticle-based DSSCs (the values increased from 2.02 ± 0.11 to 8.16 ± 0.51 mA/cm<sup>2</sup> and from 1.07 ± 0.21% to 3.88 ± 0.33%, respectively). This improvement is due to an increase in the amount of inorganic dye (N719) adsorption in the mesoporous TiO<sub>2</sub> nanoparticles with a specific surface area of 184 m<sup>2</sup>/g and an average pore size of 5 nm. These specially designed mesoporous TiO<sub>2</sub> nanoparticles have great potential as an effective dye-supporting and electron-transfer medium and can help improve the photovoltaic performance of DSSCs.

© 2012 Elsevier B.V. All rights reserved.

## 1. Introduction

Over the past few decades, dye-sensitized solar cells (DSSCs) have been developed extensively because of the relatively low costs involved in the manufacturing process compared to silicon-based solar cells. A DSSC is mainly composed of (i) a semiconductor nanocrystalline film covered with a molecular dye layer (i.e., photoanode), (ii) a redox couple in an electrolyte solution, and (iii) a platinum-based transparent conducting oxide electrode as a counter electrode. Among those, the photoanode usually consists of a TiO<sub>2</sub> nanocrystalline layer, which supports dye molecules with

absorbing light energy, especially in the visible wavelength region of sunlight. When a DSSC is exposed to sunlight irradiation of a suitable energy, electrons are excited from highest occupied molecular orbital (HOMO) to lowest unoccupied molecular orbital (LUMO) in the dye molecules. The excited electrons are subsequently injected into the conduction band of TiO<sub>2</sub> and reached to the conducting oxide electrode (e.g., fluorine-doped tin oxide, FTO). Then, the electrons flow through the external circuit and re-introduce into the DSSC on the counter electrode, flowing into the electrolyte. The electrolyte finally transports the electrons to the dye molecules, which enable to facilitate the completion of a current cycle in DSSCs [1–3].

In order to improve the overall power conversion efficiency (PCE) of DSSCs, many research groups have attempted to develop suitable dyes and reduce the interfacial resistance between TiO<sub>2</sub> particles [4–7], between the TiO<sub>2</sub> layer and the conducting electrode [8], or between the counter electrode and electrolyte [9,10].

\* Corresponding authors.

E-mail addresses: [jwkang@kims.re.kr](mailto:jwkang@kims.re.kr) (J.-W. Kang), [sookim@pusan.ac.kr](mailto:sookim@pusan.ac.kr) (S.H. Kim).

<sup>1</sup> Contributed equally to this research as co-first authors.

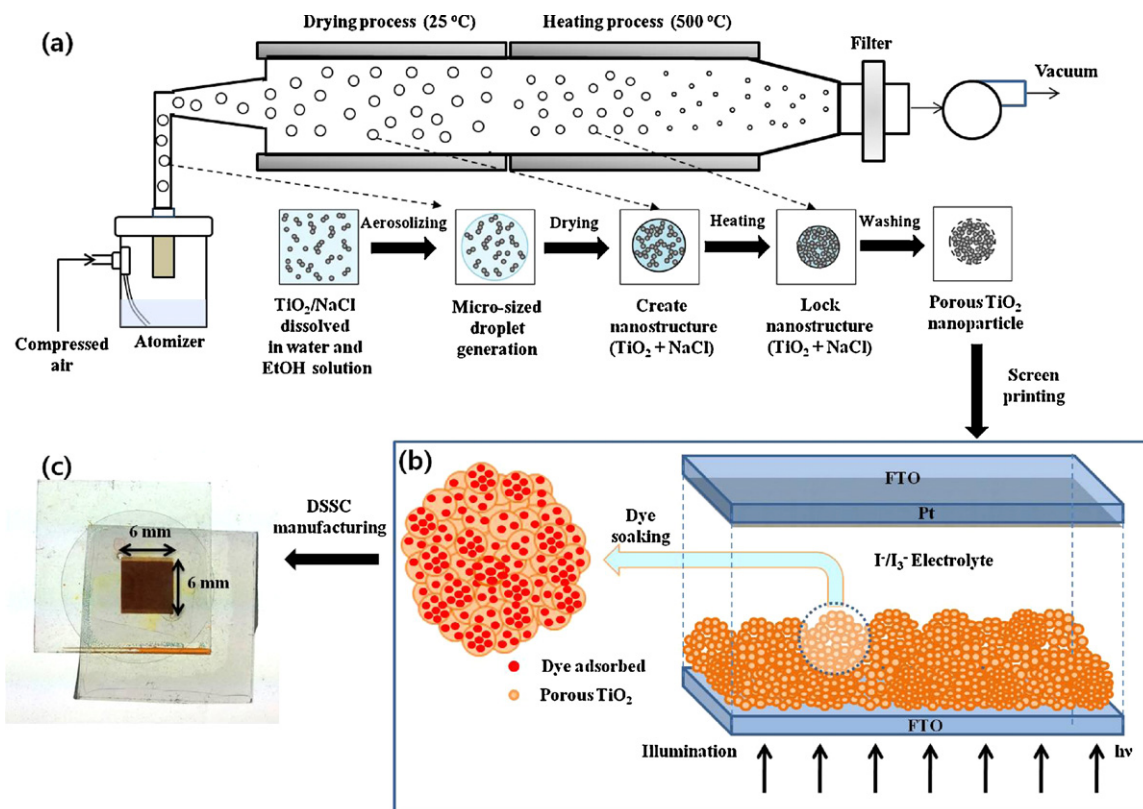


**Fig. 1.** (a) Schematic illustration of the setup for the fabrication of mesoporous  $\text{TiO}_2$  nanoparticles and the mechanism of nanoparticle formation and (b) schematic of mesoporous  $\text{TiO}_2$ -based DSSC and (c) the picture of DSSC manufactured in this study.

These previous studies have mostly focused on improving electron transfer at the various interfaces between the  $\text{TiO}_2$  layer, electrode, and electrolyte by reducing interfacial contact resistance. However, in order to achieve an inherent increase in the PCE of DSSCs, it is necessary to increase of the initial amount of dyes on a given  $\text{TiO}_2$  layer to enhance the number of electrons generated from these dyes by sunlight irradiation.

Recently, Koo et al. employed nano-embossed hollow  $\text{TiO}_2$  particles to increase the amount of dye attached on the  $\text{TiO}_2$  particles by increasing the specific surface area through a simple solvothermal reaction, without the addition of any templates or surfactants [11]. However, due to the insignificant increase in the specific surface area of such nano-embossed hollow  $\text{TiO}_2$  particles (i.e.,  $S_{\text{BET}} = \sim 58 \text{ m}^2/\text{g}$ , where  $S_{\text{BET}}$  is the specific surface area determined by nitrogen adsorption using a BET system), the amount of dye adsorption by these hollow  $\text{TiO}_2$  particles was found to be very similar to that of commercial P-25  $\text{TiO}_2$  (i.e.,  $S_{\text{BET}} = \sim 48 \text{ m}^2/\text{g}$ ). Koo et al. suggested that the hollow  $\text{TiO}_2$  particles played a key role as a light-scattering medium, which enhanced the incident light scattering and absorption in the photoanodes of DSSCs.

Unlike previous studies [12,13] on porous photoanodes formed by accumulated solid  $\text{TiO}_2$  nanoparticles, we employed a simple and inexpensive inorganic-template aero-sol-gel method to fabricate mesoporous  $\text{TiO}_2$  nanoparticles. Mesoporous  $\text{TiO}_2$  nanoparticles have nanosized pores inside, and they thus have a rather large specific surface area; as a result, they can support a high initial concentration of dye molecules in the photocatalytic active layer of DSSCs. In this work, the influence of mesoporous structures inside the  $\text{TiO}_2$  nanoparticles on the photovoltaic performance of DSSCs was systematically investigated in terms of the amount of dye molecules adsorbed, the open-circuit voltage, the short-circuit current, the fill factor, and the PCE.

## 2. Experimental

### 2.1. Aero-sol-gel synthesis of mesoporous $\text{TiO}_2$ nanoparticles

Fig. 1 presents the schematic of experimental setup for the fabrication of mesoporous  $\text{TiO}_2$  nanoparticles [14]. Briefly, two groups of precursor solutions were prepared. First, various amounts of NaCl were completely dissolved in distilled water (90 mL) in a vial, and then titanium butoxide ( $\text{C}_{16}\text{H}_{40}\text{O}_4\text{Ti}$ , 17.15 mL) was added to EtOH (72.85 mL) in another vial. The solutions were then mixed together, and the resulting mixture was ultrasonicated for an hour. This mixed precursor solution was subsequently aerosolized by a standard atomizer operated with filtered compressed air at a pressure of 241 kN/m<sup>2</sup>. The micrometer-sized droplets containing tiny  $\text{TiO}_2$  nanoparticles formed by the sol-gel reaction, NaCl, EtOH, and deionized water were continuously passed through a silica-gel dryer, in which solidified particles were formed through solvent evaporation and adsorption. The solidified aerosol particles composed of  $\text{TiO}_2$  and NaCl were then immobilized and sintered by passing through a quartz tube reactor (2.54 cm in diameter  $\times$  30 cm in heating length) enclosed by a tube furnace heated at 500 °C. Finally, the resulting  $\text{TiO}_2$ -NaCl composite nanoparticles, collected in a membrane filter with a pore size of 200 nm, were washed with deionized water using a centrifuge (Biofuge primo, Sorvall) operated at 3600 rpm for 10 min. The centrifuge-assisted washing process was repeated twice to ensure complete removal of the NaCl templates from the  $\text{TiO}_2$ -matrix nanoparticles.

### 2.2. Fabrication of DSSCs

A  $\text{TiO}_2$ -nanoparticle thin film as a photocatalytic active layer was formed by a screen-printing process on fluorine-doped tin

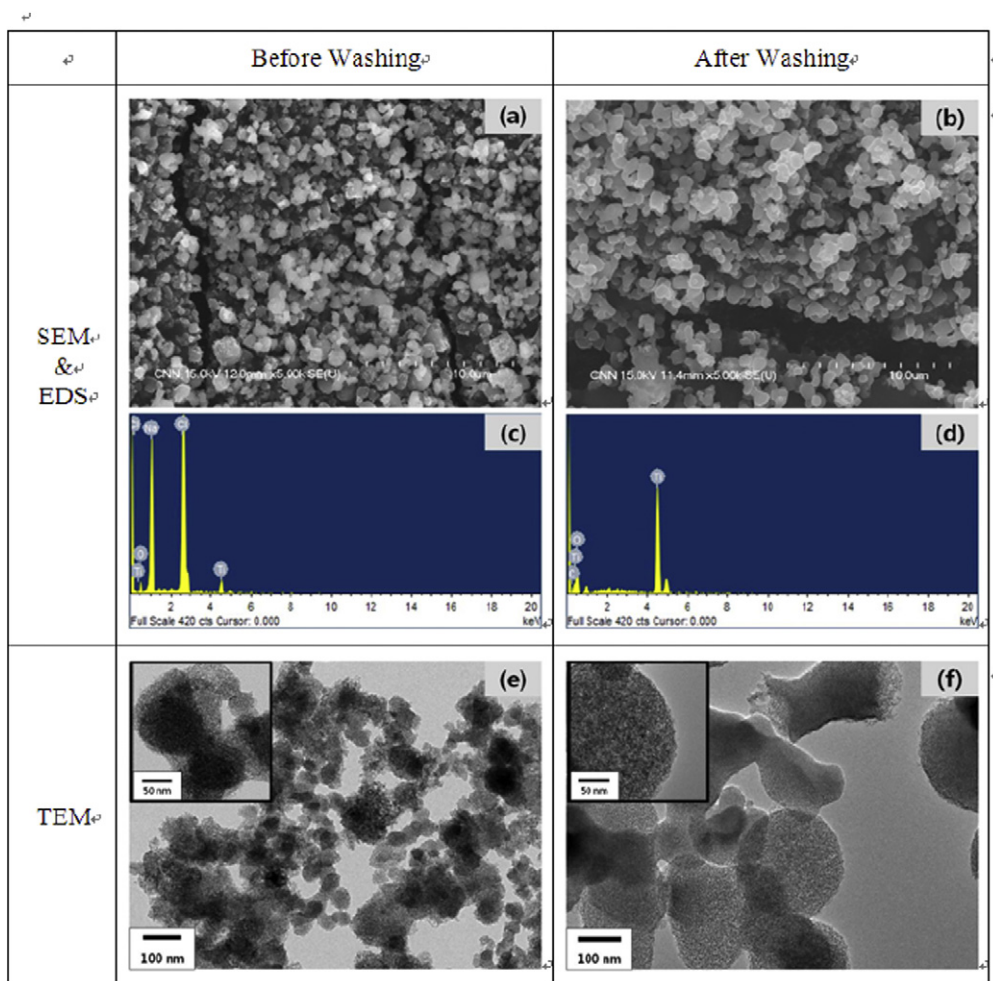


**Fig. 2.** SEM images and EDS analyses of  $\text{TiO}_2$ -NaCl composite nanoparticles (a and c) before and (b and d) after aqueous washing process. TEM images of  $\text{TiO}_2$ -NaCl composite nanoparticles (e) before and (f) after aqueous washing process. ( $\text{TiO}_2$ :NaCl = 1:5.)

oxide (FTO) glass (Pilkington,  $\text{SnO}_2$ :F,  $7 \Omega/\text{sq}$ ) with an active area of  $0.6 \text{ cm} \times 0.6 \text{ cm}$ . The optimized thickness of  $\text{TiO}_2$  nanoparticle layer was experimentally determined to be  $18 \pm 2 \mu\text{m}$ , which made the best power conversion efficiency (PCE) of DSSCs assembled in this study. As we increased the thickness of  $\text{TiO}_2$  nanoparticle layer  $>18 \pm 2 \mu\text{m}$ , the PCE of DSSCs began to decrease due to the significant reduction of light transmittance. In order to prepare  $\text{TiO}_2$  paste for the screen-printing process, 17 g of mesoporous  $\text{TiO}_2$  nanoparticles fabricated in this study and 23 g of citric acid dispersed in 29 g ethylene glycol were mixed in a vial.

The  $\text{TiO}_2$ -nanoparticle layer formed on the FTO glass by screen-printing process was then sintered at  $500^\circ\text{C}$  for 30 min and subsequently immersed in anhydrous ethanol containing 0.5 mM Ru-dye ( $\text{Bu}_4\text{N}$ ) $_2$ [Ru(Hdcbpy) $_2$ -(NCS) $_2$ ] (N719 dye, Solaronix), and it was kept for 24 h at room temperature in order to allow the dye molecules to become attached to the entire surface and to available inner pores of the  $\text{TiO}_2$  nanoparticles. The dye-soaked  $\text{TiO}_2$ -nanoparticle layer electrode was then rinsed with ethanol and dried in a convection oven at  $80^\circ\text{C}$  for 10 min. As a counter electrode, we prepared Pt-coated FTO glass using an ion-sputter (E1010, Hitachi) operated at 2.5 kV. Both the dye-soaked  $\text{TiO}_2$ -layer photoanode and Pt-coated counter electrode were sealed together with an inserted hot-melt polymer film (60  $\mu\text{m}$  thickness, Surlyn, DuPont), and an iodide-based liquid electrolyte (AN-50, Solaronix) was then injected into the interspace between the electrodes.

### 2.3. Characterization of materials and photovoltaic devices

The morphologies of the resulting mesoporous  $\text{TiO}_2$  nanoparticles synthesized by the aero-sol-gel process employed in this study were characterized using scanning electron microscopy (SEM, S-4200, Hitachi) operated at  $\sim 15 \text{ kV}$  and transmission electron microscopy (TEM, JEM 2100F, JEOL) operated at  $\sim 100 \text{ kV}$ . The specific surface area and pore size distribution of mesoporous  $\text{TiO}_2$  nanoparticles were characterized by analyzing the  $\text{N}_2$  adsorption and desorption isotherms obtained at 77 K using Quadrasorb-SI equipment (Quantachrome, UK). All the  $\text{TiO}_2$  nanoparticles fabricated in this approach were degassed at  $200^\circ\text{C}$  and  $10^{-6}$  Torr for 8 h prior to the specific surface area and pore size distribution measurements. The specific surface areas of the  $\text{TiO}_2$  nanoparticles were calculated with the Brunauer-Emmett-Teller (BET) equation, and their pore size distributions were determined by using the Barrett-Joyner-Halenda (BJH) formula from the desorption branch.

In order to evaluate the amount of dye adsorption, the dye molecules were first desorbed from the  $\text{TiO}_2$  layer by rinsing with 0.1 M aqueous NaOH solution (water:EtOH = 1:1). Then, the light absorbance of the dye-containing solution was measured using a Scan UV-vis spectrophotometer (CARY<sup>®</sup> 5000, Varian, Inc.). The current density-voltage ( $J$ - $V$ ) characteristics of the DSSCs were measured under AM 1.5 simulated illumination with an intensity of  $100 \text{ mW}/\text{cm}^2$  (PEC-L11 model, Pecell Technologies Inc.). The intensity of sunlight illumination was calibrated using a standard

Si photodiode detector with a KG-5 filter. The  $J$ - $V$  curves were recorded automatically with a Keithley SMU 2400 source meter by illuminating the DSSCs.

### 3. Results and discussion

Hybrid  $\text{TiO}_2$ -NaCl composite nanoparticles were formed using the aero-sol-gel process employed in this study. The salt templates present inside the  $\text{TiO}_2$ -matrix nanoparticles were expected to prevent the thermal shrinkage of the  $\text{TiO}_2$  structure introduced into the tube furnace reactor, thus playing a key role in securing the pore structures before aqueous salt removal. The hybrid  $\text{TiO}_2$ -NaCl composite nanoparticles were finally transformed into mesoporous  $\text{TiO}_2$  nanoparticles by removing the salts through a subsequent aqueous washing process. The formation of mesoporous  $\text{TiO}_2$  nanoparticles and aqueous removal of salt templates ( $\text{TiO}_2$ :NaCl = 1:5) were confirmed by SEM, EDS, and TEM analyses, as shown in Fig. 2. SEM images of as-prepared  $\text{TiO}_2$ -NaCl composite nanoparticles show spherical, loosely aggregated particles as shown in Fig. 2a. Following salt removal by aqueous washing process, there was no appreciable change in the overall structure of the resulting  $\text{TiO}_2$  nanoparticles as shown in Fig. 2b. This suggests that salt templates homogeneously distribute inside  $\text{TiO}_2$  matrix nanoparticles. Complete salt removal by aqueous washing process was confirmed by EDS analysis as shown in Fig. 2c and d. One can easily see the strong signals of  $\text{TiO}_2$  and NaCl for the as-prepared  $\text{TiO}_2$ -NaCl composite nanoparticles (Fig. 2c), while the signals of NaCl completely disappeared after aqueous washing process (Fig. 2d). From the TEM results as shown in Fig. 2e, the average diameter of as-prepared  $\text{TiO}_2$ -NaCl composite nanoparticles was approximately  $\sim 200$  nm. However, the  $\text{TiO}_2$  nanoparticles formed by the combination of aero-sol-gel and aqueous washing processes were clearly observed to have porous inner structures without marked differences in overall structure of the particles as shown in Fig. 2f, indicating that salt did reside within the particle interior.

The effect of mixing ratio between  $\text{TiO}_2$  and NaCl on the pore structure in the resulting  $\text{TiO}_2$  nanoparticles is presented in Fig. 3. We note that the specific surface area of mesoporous  $\text{TiO}_2$  nanoparticles suddenly increased with a relatively small salt fraction up to a mixture ratio of  $\text{TiO}_2$ :NaCl = 1:1 from 1:0, which suggests that the salt filler began supporting the porous network inside the  $\text{TiO}_2$  nanoparticles. However, increasing the salt mass fraction further (to more than the ratio of  $\text{TiO}_2$ :NaCl = 1:1) resulted in a decrease in the specific surface area, as shown in Fig. 3a. With larger salt mass fractions, the  $\text{TiO}_2$ -NaCl composite nanoparticles had larger salt precipitates, which presumably resulted in the formation of smaller pore volumes, and thereby decreasing the surface area of the  $\text{TiO}_2$  nanoparticles upon salt removal. This fact was also confirmed by the BET measurements of pore size distributions of  $\text{TiO}_2$  nanoparticles as a function of salt mass fraction, as shown in Fig. 3b. The maximum specific surface area of mesoporous  $\text{TiO}_2$  nanoparticles fabricated in this approach was found to be approximately  $278 \text{ m}^2/\text{g}$  for the mixture ratio of  $\text{TiO}_2$ :NaCl = 1:1. It should also be noted that with very high salt mass fractions (e.g.,  $\text{TiO}_2$ :NaCl = 1:10), there was no formation of porous  $\text{TiO}_2$  structures with sufficient rigidity. Instead, it was found that fractured solid  $\text{TiO}_2$  nanoparticles were formed following the aqueous washing process.

X-ray diffraction patterns are shown in Fig. 4 for the as-prepared and washed powder composed of  $\text{TiO}_2$  and NaCl with a ratio of 1:5. For the as-prepared powder (i.e.,  $\text{TiO}_2$ -NaCl composite nanoparticles), the spectra show very strong diffraction from NaCl (Fig. 4a). However, after aqueous wash and subsequent calculation for the  $\text{TiO}_2$ -NaCl composite particles (i.e., mesoporous  $\text{TiO}_2$  nanoparticles), one can see the strong peaks corresponding to highly crystallized anatase structure of  $\text{TiO}_2$  without any impurity phase

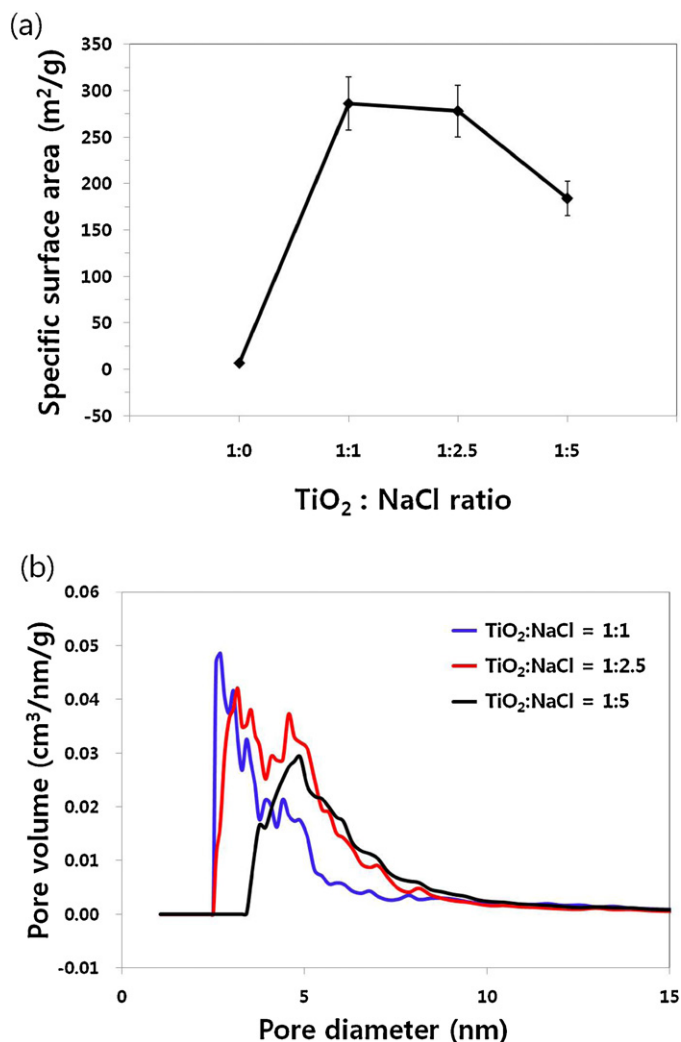


Fig. 3. (a) Specific surface areas (SSAs) and (b) pore size distributions of the mesoporous  $\text{TiO}_2$  nanoparticles synthesized by varying the mass fraction of NaCl in the  $\text{TiO}_2$ -NaCl composite nanoparticles.

(Fig. 4b) with a crystallite size estimated using Scherrer's equation of 15 nm.

In order to examine the effect of the mesoporous  $\text{TiO}_2$  nanoparticle structure on the dye adsorption, various photoanodes with a fixed photoactive area of  $0.6 \text{ cm} \times 0.6 \text{ cm}$  were constructed with the mesoporous  $\text{TiO}_2$  nanoparticles synthesized using our approach. The use of the mesoporous  $\text{TiO}_2$  nanoparticles in the photoanode of DSSCs can provide a sufficient surface area for the dye attachment. For the evaluation of the amount of dye attached to the  $\text{TiO}_2$  layer in the photoanode of the DSSCs, the light absorbance of the desorbed dye solution was measured using a UV-vis spectrometer [11]. The desorbed dye solution was prepared by immersing the N719 dye-sensitized photoanode in aqueous NaOH solution (0.1 M) to completely desorb the dye molecules. The amount of dye adsorbed was then calculated using the Beer-Lambert law. Table 1 presents the amount of dye adsorption in various  $\text{TiO}_2$  layers in the photoanode of the DSSCs, the specific surface area of the  $\text{TiO}_2$  nanoparticles, and the performance of the DSSCs. One can clearly see that the specific surface area of mesoporous  $\text{TiO}_2$  nanoparticles synthesized using this approach reached its maximum (i.e.,  $\text{SSA} = 286 \text{ m}^2/\text{g}$ ) at a mixture ratio of  $\text{TiO}_2$ :NaCl = 1:1, and then began to decrease with increasing salt mass fraction. However, the amount of dye adsorption showed quite the opposite trend. In other words, the amount of dye adsorption unexpectedly

**Table 1**  
Summary of specific surface area, dye adsorption, and photovoltaic characteristics of TiO<sub>2</sub>.

| Type of TiO <sub>2</sub> | TiO <sub>2</sub> :NaCl ratio | Specific surface area (m <sup>2</sup> /g) | Average pore size (nm) | Dye adsorption (10 <sup>-7</sup> mol/cm <sup>2</sup> ) | <i>J</i> <sub>sc</sub> (mA/cm <sup>2</sup> ) | <i>V</i> <sub>oc</sub> (V) | FF          | PCE (%)     |
|--------------------------|------------------------------|---|------------------------|--|--|----------------------------|-------------|-------------|
| Solid TiO <sub>2</sub>   | 1:0                          | 7   | –                      | 0.12   | 2.02 ± 0.11                                  | 0.71 ± 0.02                | 0.74 ± 0.03 | 1.07 ± 0.05 |
| Porous TiO <sub>2</sub>  | 1:1                          | 286                                       | 1.9                    | 0.14   | 2.59 ± 0.19                                  | 0.72 ± 0.01                | 0.73 ± 0.02 | 1.37 ± 0.14 |
| Porous TiO <sub>2</sub>  | 1:2.5                        | 278                                       | 3.1                    | 0.31   | 2.95 ± 0.24                                  | 0.71 ± 0.01                | 0.73 ± 0.02 | 1.53 ± 0.10 |
| Porous TiO <sub>2</sub>  | 1:5                          | 184                                       | 4.8                    | 1.37   | 8.16 ± 0.51                                  | 0.72 ± 0.02                | 0.66 ± 0.03 | 3.88 ± 0.33 |

*J*<sub>sc</sub> = short circuit current, *V*<sub>oc</sub> = open circuit voltage, FF = fill factor, PCE = power conversion efficiency.

reached its maximum (i.e., DA = 1.37 × 10<sup>-7</sup> mol/cm<sup>2</sup>, where DA is the amount of dye adsorption) at a moderate specific surface area (i.e., SSA = 184 m<sup>2</sup>/g, APS = ~5 nm, where, SSA denotes the specific surface area and APS represents the average pore size) of mesoporous TiO<sub>2</sub> nanoparticles formed at a mixture ratio of TiO<sub>2</sub>:NaCl = 1:5. The amount of dye adsorption then decreased significantly as the specific surface area increased for the mesoporous TiO<sub>2</sub> nanoparticles formed at the mixture ratios of TiO<sub>2</sub>:NaCl = 1:1 (DA = 0.14 × 10<sup>-7</sup> mol/cm<sup>2</sup>, SSA = 286 m<sup>2</sup>/g, APS = ~2 nm) and TiO<sub>2</sub>:NaCl = 1:2.5 (DA = 0.31 × 10<sup>-7</sup> mol/cm<sup>2</sup>, SSA = 278 m<sup>2</sup>/g,

APS = ~3 nm), respectively, indicating that to some extent, the amount of dye adsorption increased significantly with increasing salt mass fractions in the TiO<sub>2</sub>-NaCl composite nanoparticles. This is presumably because a sufficient pore size is required for the dye molecules to penetrate and adsorb inside the mesoporous TiO<sub>2</sub> nanoparticles. It is well known that N-719 dye has a crystal triclinic structure (*a* = 1.15 nm, *b* = 1.26 nm, *c* = 1.90 nm) and the thickness of the dye layer attached to the TiO<sub>2</sub> particles is 1–2 nm [15]. When the average pore size of mesoporous TiO<sub>2</sub> nanoparticles is comparable to or smaller than that of dye molecules, the dye molecules are not able to penetrate through the pores, and as a result, the amount of dye adsorption inside the pore structures of TiO<sub>2</sub> is significantly decreased. Therefore, the optimized conditions in terms of both specific surface area and pore size should be determined in order to increase the amount of dye adsorption in the mesoporous TiO<sub>2</sub> particles.

In order to examine the effect of mesoporous TiO<sub>2</sub> nanoparticles on the photovoltaic performance of DSSCs, we fabricated DSSCs composed of various mesoporous TiO<sub>2</sub> nanoparticles synthesized by the aero-sol-gel process. Table 1 and Fig. 5 summarize the photovoltaic characteristics and current-voltage (*J*-*V*) curves of the fabricated DSSCs measured under AM 1.5 illumination (100 mW/cm<sup>2</sup>) as a function of the mass fraction of NaCl present in the TiO<sub>2</sub>-NaCl composite nanoparticles. For different mass fractions of NaCl in the TiO<sub>2</sub>-NaCl nanoparticles, the short circuit current (*J*<sub>sc</sub>) increased with increasing mass fraction of NaCl in the mesoporous TiO<sub>2</sub> nanoparticle-based photoanodes in DSSCs. The *J*<sub>sc</sub> values of DSSCs composed of mesoporous TiO<sub>2</sub> nanoparticles increased from 2.59 ± 0.19 mA/cm<sup>2</sup> for TiO<sub>2</sub>:NaCl = 1:1 to 8.16 ± 0.51 mA/cm<sup>2</sup> for TiO<sub>2</sub>:NaCl = 1:5, resulting in a considerable improvement of the PCE from 1.37 ± 0.14% to 3.88 ± 0.33%, respectively. The increase in electron concentration resulted from the use of the mesoporous TiO<sub>2</sub> nanoparticles with relatively high specific surface area and sufficiently large pore size, which enabled

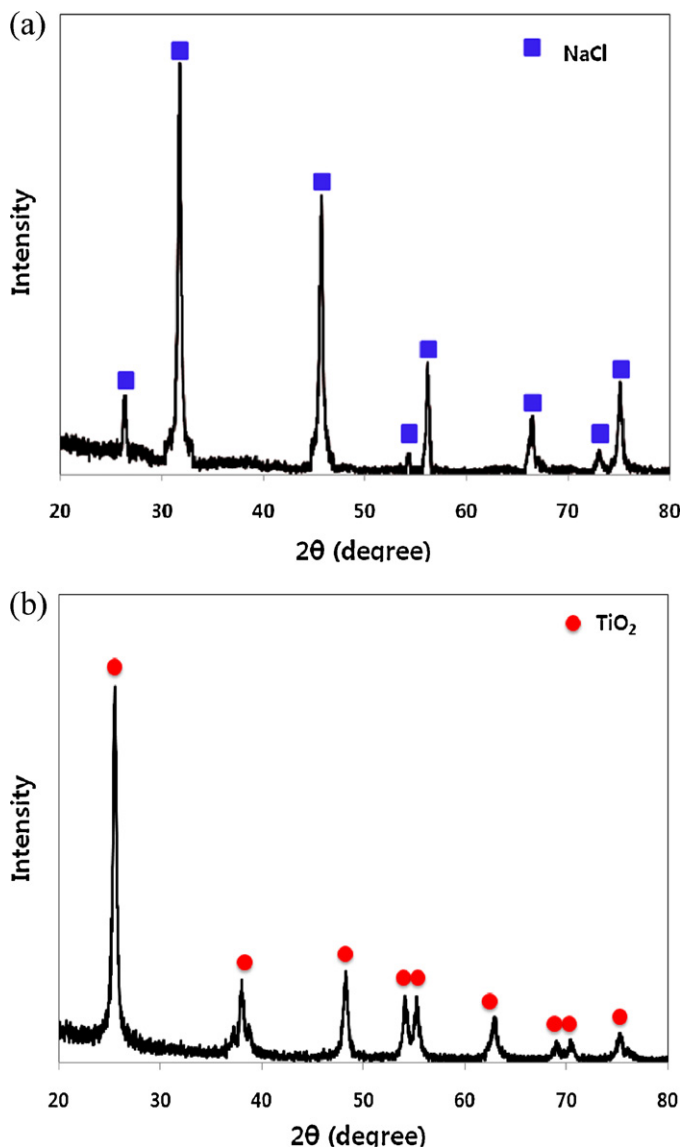


**Fig. 4.** XRD patterns of (a) as-prepared TiO<sub>2</sub>-NaCl composite nanoparticles (TiO<sub>2</sub>:NaCl = 1:5) and (b) post aqueous washed and subsequently calcined mesoporous TiO<sub>2</sub> nanoparticles.

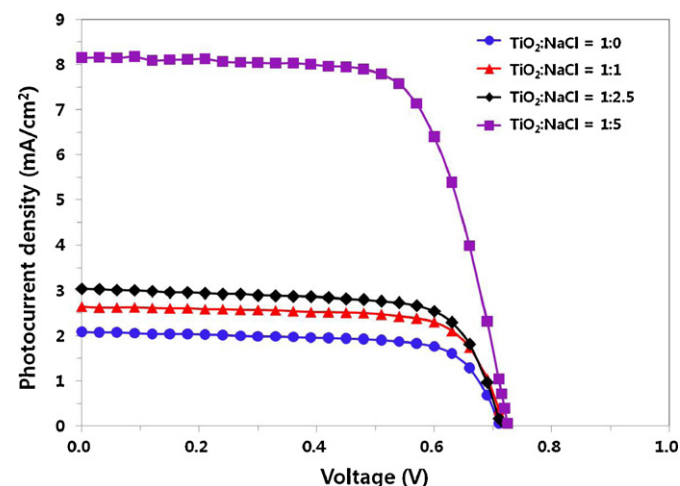


**Fig. 5.** *J*-*V* characteristics of solid TiO<sub>2</sub> nanoparticles (TiO<sub>2</sub>:NaCl = 1:0)- and mesoporous TiO<sub>2</sub> nanoparticles (TiO<sub>2</sub>:NaCl = 1:1, 1:2.5, and 1:5)-based DSSCs.

the adsorption of a larger number of dye molecules; this was a major factor responsible for improving both  $J_{sc}$  and the PCE of DSSCs. However, it is to be noted that both the open circuit voltage ( $V_{oc}$ ) and fill factor (FF) of the DSSCs constructed with mesoporous  $TiO_2$  nanoparticles did not show any appreciable changes even compared with those of DSSCs constructed with solid  $TiO_2$  nanoparticles (i.e.,  $TiO_2:NaCl = 1:0$ ). This suggests that the photoelectric conversion properties of the solid  $TiO_2$  nanoparticles and those of our synthesized mesoporous  $TiO_2$  nanoparticles were very similar. An increase in  $J_{sc}$  accounts for the best PCE of  $3.88 \pm 0.33\%$  for the DSSCs constructed with the mesoporous  $TiO_2$  nanoparticles. This actually gave an improvement of 263% over the PCE of  $1.07 \pm 0.05\%$  found for the DSSCs constructed with solid  $TiO_2$  nanoparticles. Here, DSSCs composed of commercially available Degussa P-25  $TiO_2$  nanoparticles were also assembled for comparison, and it showed an improvement of about 21% over the PCE of  $3.2 \pm 0.05\%$ . Even though the amount of dye adsorption in mesoporous  $TiO_2$  nanoparticle-based DSSCs ( $DA = 1.37 \times 10^{-7}$  mol/cm<sup>2</sup>) was almost twice as high as that in Degussa P-25  $TiO_2$  nanoparticle-based DSSCs ( $DA = 0.73 \times 10^{-7}$  mol/cm<sup>2</sup>), the magnitude of the improvement in the photovoltaic performance of the mesoporous  $TiO_2$  nanoparticle-based DSSCs was rather low. Possible reasons for this are the following: (i) the light irradiation can be scattered due to the relatively large size of the mesoporous  $TiO_2$  nanoparticles (average particle diameter: approximately 200 nm), (ii) the light irradiation might not reach a sufficient depth inside the pore structures, (iii) the charge recombination inside the mesoporous  $TiO_2$  nanoparticles may increase because of the close proximity between the dye molecules, and (iv) it is difficult to ensure uniform contact of the liquid electrolyte with the surface of the nanopores formed inside the  $TiO_2$  nanoparticles.

#### 4. Conclusions

In this work, we have described a simple and viable aero-sol-gel method for the synthesis of mesoporous  $TiO_2$  nanoparticles; the method facilitates the formation of nanoparticles with a relatively high specific surface area and large pore volume that are capable of adsorbing dye molecules when used in a photoanodes of DSSCs. The photovoltaic performance of DSSCs is improved when these nanoparticles are used in the photoanodes. After a series of combined aero-sol-gel and aqueous washing processes were used for the formation of  $TiO_2$ -NaCl composite nanoparticles, various mesoporous  $TiO_2$  nanoparticles with specifically determined specific surface areas and pore volume distributions were obtained; these were then used to form a photovoltaic active layer on the photoanodes of DSSCs. Compared with the solid  $TiO_2$  nanoparticle-based DSSCs, the mesoporous  $TiO_2$  nanoparticle-based DSSCs fabricated in this study showed an improved  $J_{sc}$  and PCE values. The optimum conditions for achieving the best photovoltaic performance of DSSCs in this approach were obtained with mesoporous  $TiO_2$  nanoparticles with a specific surface area of 184 m<sup>2</sup>/g and average pore size of ~5 nm, which generated a  $V_{oc}$  of  $0.72 \pm 0.02$  V,  $J_{sc}$  of

$8.16 \pm 0.51$  mA/cm<sup>2</sup>, fill factor of  $0.66 \pm 0.03$ , and a resulting PCE of  $3.88 \pm 0.33\%$ . This suggests that the controlled synthesis of mesoporous  $TiO_2$  nanoparticles with the desired surface area and pore volume distribution for supporting a higher concentration of dye molecules has good potential for the improvement of the inherent photovoltaic performance of DSSCs.

#### Acknowledgments

This study was supported by National Research Foundation of Korea (NRF) funded by Korean government (MEST) (2011-0013114) and Busan Metropolitan City through the Project for Regional Science Park. This study was also partially supported by the Converging Research Center Program through the National Research Foundation of Korea (NRF), funded by the Ministry of Education, Science, and Technology (2009-0081928).

#### References

- [1] M. Gratzel, Dye-sensitized solar cells, *J. Photochem. Photobiol. C* 4 (2003) 145–153.
- [2] M. Ikegami, J. Suzuki, K. Teshima, M. Kawaraya, T. Miyasaka, Improvement in durability of flexible plastic dye-sensitized solar cell modules, *Sol. Energy Mater. Sol. Cells* 93 (2009) 836–839.
- [3] T. Yamaguchi, Y. Uchida, S. Agatsuma, H. Arakawa, Series-connected tandem dye-sensitized solar cell for improving efficiency to more than 10%, *Sol. Energy Mater. Sol. Cells* 216 (2010) 104–109.
- [4] R. Katoh, M. Kasuya, A. Furube, N. Fuke, N. Koide, L. Han, Quantitative study of solvent effects on electron injection efficiency for black-dye-sensitized nano crystalline  $TiO_2$  films, *Sol. Energy Mater. Sol. Cells* 93 (2009) 698–703.
- [5] V. Duprez, M. Biancardo, F.C. Krebs, Characterisation and application of new carboxylic acid-functionalised ruthenium complexes as dye-sensitisers for solar cells, *Sol. Energy Mater. Sol. Cells* 93 (2009) 698–703.
- [6] S.H. Kang, S.H. Choi, M.S. Kang, J.Y. Kim, H.S. Kim, T.G. Hyeon, Y.E. Sung, Nanorod-based dye-sensitized solar cells with improved charge collection efficiency, *Adv. Mater.* 20 (2008) 54–58.
- [7] J.H. Pan, X.S. Zhao, In Lee Wan, Block copolymer-templated synthesis of highly organized mesoporous  $TiO_2$ -based films and their photoelectrochemical applications, *Chem. Eng. J.* 170 (2011) 363–380.
- [8] Y. lu, X. Sun, Q. Tai, H. Hu, B. Chen, N. Huang, B. Sebo, X.Z. Zhao, Efficiency enhancement in dye-sensitized solar cells by interfacial modification of conducting glass/mesoporous  $TiO_2$  using a novel ZnO compact blocking film, *J. Power Sources* 196 (2011) 475–481.
- [9] X. Fang, T. Ma, G. Guan, M. Akiyama, T. Kida, E. Abe, Effect of the thickness of the Pt film coated on a counter electrode on the performance of a dye-sensitized solar cell, *J. Electroanal. Chem.* 570 (2004) 257–263.
- [10] M. Biancardo, K. West, F.C. Krebs, Quasi-solid-state dye-sensitized solar cells: Pt and PEDOT:PSS counter electrodes applied to gel electrolyte assemblies, *J. Photochem. Photobiol. A* 187 (2007) 395–401.
- [11] H.J. Koo, Y.J. Kim, Y.H. Lee, W.I. Lee, K. Kim, N.G. Park, Nano-embossed hollow spherical  $TiO_2$  as bifunctional material for high-efficiency dye-sensitized solar cells, *Adv. Mater.* 20 (2008) 195–199.
- [12] L. Hu, S. Dai, J. Weng, S. Xiao, Y. Sui, Y. Huang, S. Chen, F. Kong, X. Pan, L. Liang, K. Wang, Microstructure design of nanoporous  $TiO_2$  photoelectrodes for dye-sensitized solar cell modules, *J. Phys. Chem. B* 111 (2007) 358–362.
- [13] S. To, T.N. Murakami, P. Comte, P. Liska, C. Gratzel, M.K. Nazeeruddin, M. Gratzel, Fabrication of thin film dye sensitized solar cells with solar to electric power conversion efficiency over 10%, *Thin Solid Films* 516 (2008) 4613–4619.
- [14] S.H. Kim, B.Y.H. Liu, M.R. Zachariah, Synthesis of nanoporous metal oxide particles by a new inorganic matrix spray pyrolysis method, *Chem. Mater.* 14 (7) (2002) 2889–2899.
- [15] Y. Yoshioka, M. Tsujimoto, M. Koshino, T. Nemoto, T. Ogawa, H. Kurata, S. Isoda, Characterization of Gratzel dye on  $TiO_2$  particles by transmission electron microscopy, *Mol. Cryst. Liq. Cryst.* 424 (2004) 95–102.